American Mineralogist, Volume 59, pages 947–963, 1974

Controlled Nucleation and Crystal Growth of Various $CaCO_3$ Phases by the Silica Gel Technique

JAMES W. MCCAULEY[1], AND RUSTUM ROY

Department of Geochemistry and Mineralogy and the Materials Research Laboratory, The Pennsylvania State University, University Park, Pennsylvania 16802

Abstract

The effect of the environment on the precipitation and crystal growth of $CaCO_3$ from aqueous solutions at ordinary temperature and pressure has been investigated using the silica gel technique. Thermodynamics fails to predict many of the observed assemblages, suggesting that kinetic mechanisms are more important for these quasi-metastable occurrences. The effect of concentration of reactants, pH, and impurity ions on the precipitation of $CaCO_3$ in a silica gel has been determined. Aragonite formation, in the absence of impurity cations, seems to be caused by the entrapment of HCO_3^-, which is a function of the relative concentration of CO_3^{2-} to HCO_3^-. Synthesis data for vaterite suggests that this phase may be related to the precursor formation of $CaCO_3 \cdot H_2O$ and also that it is not a stoichiometric $CaCO_3$ phase; rather, a Ca-rich material with small incorporations of (OH), HCO_3, or CO_2 (aq.). The morphology of calcite and aragonite, in the absence of impurity cations, is a pronounced function of pH. In the presence of the impurity cations, Sr^{2+}, Mg^{2+}, and Ni^{2+}, aragonite formation is controlled by its epitaxial growth on aragonite-like nuclei; for Sr^{2+} unequivocal evidence indicates that this nucleus is $SrCO_3$, whereas, for Mg the nucleus seems to be $MgCO_3 \cdot 3H_2O$, nesquehonite.

The partition of these impurity cations between solution and the various precipitating solids is a complex function of pH, relative concentration of reactants and impurity ions, and amounts of various $CaCO_3$ phases precipitating simultaneously. The partition coefficients for Sr in aragonite and calcite were 4.37 and 1.04 respectively. Single crystals of calcite, with 7.5 mole percent Mg, were grown by this technique.

Introduction

Calcium carbonate precipitation from aqueous solution is affected in varying degree by the environment, but the mechanisms are still somewhat obscure and unverified by direct evidence. Five polymorphic modifications of crystalline anhydrous $CaCO_3$, each with a fairly well defined temperature and pressure field of stability, have been described: calcite I (hereinafter called calcite), calcite II, calcite III, aragonite, and vaterite. However, calcite, aragonite, and vaterite may be prepared either singly or simultaneously by precipitation from an aqueous solution at ordinary temperature and pressure conditions, even though only calcite is thermodynamically stable. The metastable formation of vaterite and aragonite at room conditions results from interferences in the equilibrium process by kinetic considerations. Many reviews of this problem have been published: Goto (1961), Fisher (1962), Bricker and Garrels (1967), *etc.*

Most of the investigations in this area have been concerned with the effect of impurity ions on the phase that separates from solution. Johnston, Merwin, and Williamson (1916), in an early classic work, showed that when Pb was added to the precipitating medium aragonite formed; these crystals had an optically distinct nucleus, which appeared to be $PbCO_3$, suggesting epitaxial control. Since then, other workers (Murray, 1954; Wray and Daniels, 1957; Zeller and Wray, 1956; Kitano, 1962, 1964; Kitano and Hood, 1962; Simkiss, 1964; Bischoff and Fyfe, 1968) have shown how other cations such as Sr, Mg, and Ba affect calcite and aragonite formation. MacDonald (1956) calculated thermodynamically that at least 30 mole percent of a typical impurity ion (*e.g.*, Sr) in crystalline solution is needed to stabilize the formation of

[1] Now at the Army Materials and Mechanics Research Center, Watertown, Massachusetts 02172.

aragonite in the calcite stability field. Using a unique concept of adjusting the dielectric constant of various $CaCO_3$ precipitation environments, Goto (1961) analyzed the question in terms of hydration energies of the ions. His results, although quite interesting, seem inconsistent with those of other workers.

The influence of Sr and Ba should be very similar to that of Pb as described by Johnston, Merwin and Williamson (1916), and this has been confirmed in general. Mg, however, also favors aragonite formation, although somewhat anomalously. Lippmann (1960) proposed that Mg poisons the growing calcite crystals, thus allowing for the eventual supersaturation and precipitation of aragonite. Bischoff (1968a) also has established the tendency for Mg to poison growth. Buerger (1971) has suggested that Sr can influence the precipitation of aragonite over calcite, by providing nuclei with an aragonite structure.

In general, analyses of natural $CaCO_3$ polymorphs for trace elements (Siegel, 1961; Stehli and Hower, 1961) and laboratory investigations (Oxburgh, Segnit, and Holland, 1959; Holland *et al*, 1963, 1964) indicate that calcite is generally higher in Mg and lower in Sr, Ba, and Pb than is aragonite.

Aragonite formation also seems to be favored by high pH and high water temperature (greater than 70°C). But here again, few hypotheses concerning the mechanisms involved have been offered.

Vaterite has always been a special problem, in that it has a vastly different crystal structure than calcite and aragonite (Meyer, 1969), and because until recently it had no known *T-P* stability region. Its natural (McConnell, 1960) and laboratory occurrence has always been quite intriguing. The formation of vaterite is promoted by the presence of barium (Kitano, 1962; Goto, 1961) and by water temperatures of 40°–70°C (Kitano and Hood, 1962; Johnston, Merwin, and Williamson, 1916; and Dekeyser and Degueldre, 1950). Dekeyser and Degueldre (1950) have also shown that almost 100 percent vaterite is formed when $CaCl_2$ is added to Na_2CO_3, but when Na_2CO_3 is added to $CaCl_2$, almost 100 percent calcite precipitates.

Classical low temperature experimental techniques have shed much light on these problems, but have also created some new ones. In these techniques, reaction and precipitation normally proceed very rapidly, usually with formation of crystals much too small for individual study. Preliminary experimentation using a silica gel technique (Vand, Henisch, and McCauley, 1963) for the crystal growth of various slightly soluble materials, including $CaCO_3$, indicated that this technique would be particularly adaptable to $CaCO_3$ problems. During this initial work, our first attempt to grow crystals of $CaCO_3$ resulted in the formation of all three $CaCO_3$ polymorphs side by side in the test tube. Spurred on by these preliminary results, a detailed study was initiated to examine the synthesis of $CaCO_3$ in controlled environments (McCauley, 1965). After McCauley and Roy (1965, 1966a, b) described the silica gel crystal growth of $CaCO_3$ and $SrSO_4$, several other investigators re-examined the crystal growth of $CaCO_3$ in gels (Nickel and Henisch, 1969; Barta and Zemlicka, 1971; Schwartz *et al*, 1971). An extensive literature survey revealed that Fisher and Simons (1962a, b) and Morse and Donnay (1931) were the first to grow crystals of $CaCO_3$ in a gel.

These initial studies demonstrated that fairly large crystals may be routinely prepared, and then separated and studied independently by various techniques. Even more intriguing is that the crystals may be observed during their nucleation and growth either macroscopically or microscopically since the gel is optically transparent. Further, the pH and the concentration of reactants and impurity ions can also be independently adjusted. Moreover, extraneous effects on the precipitates are minimized since early formed nuclei are delicately held in the position of their formation, separate from all other first formed nuclei. This minimizes effects due to precipitate-precipitate interaction and crystal impact on the bottom of the container. The data obtained, then, should yield information concerning the *mechanisms* which operate to alter the predicated equilibrium assemblage of phases and the occurrence, both natural and synthetic, of the various $CaCO_3$ polymorphs.

Experimental Method

The use of gels as a reaction medium has received sporadic attention since 1896 when R. E. Liesegang first observed the periodic precipitation of slightly soluble salts in gelatin. "Liesegang Rings" inspired many chemists and mineralogists to study other reactions in various colloids; among the early workers was Holmes (1917), who successfully grew fairly large crystals of a variety of materials.

The technique can be described as crystal growth by reaction; two solutions of soluble salts are

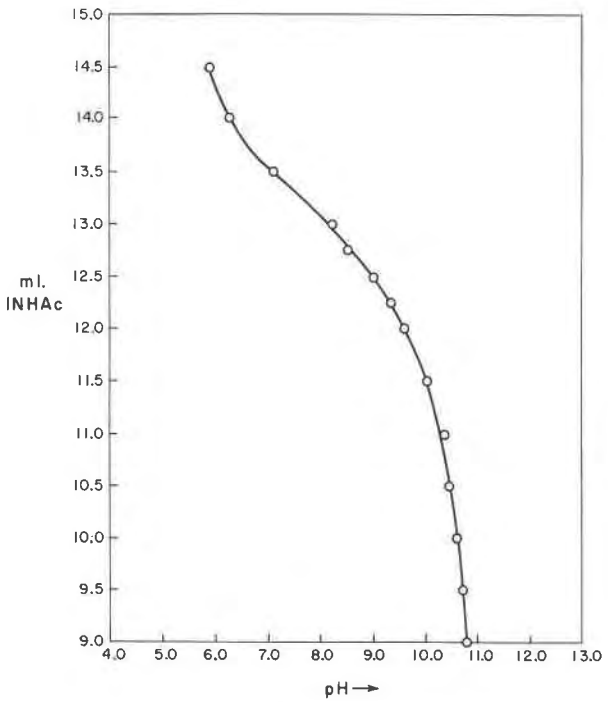

FIG. 1. Titration curve for 10 ml 0.75 molal $Na_2SiO_3:9H_2O$ at 28°C.

brought together by diffusion through a gel with subsequent nucleation and crystal growth taking place by precipitation of a reaction-formed supersaturated phase within the gel. Various mechanisms have been suggested to describe the function of the gel in the crystal growth process. In general, however, the gel limits the number of critical-size nuclei that are formed and decreases the rate of growth by controlling diffusion of the reacting ions and, more importantly, by governing the speed of reaction at the crystal's growing surface. The gel is assumed to be chemically inert to any reaction that takes place and may be thought of as analogous to a glass sponge. For more details and discussions of these mechanisms see McCauley (1965) and Henisch (1970).

A gel may be formed using a wide variety of techniques and materials; in this work silicic acid gel was prepared by the acidification of aqueous solutions of $Na_2SiO_3 \cdot 9H_2O$ (Fisher Scientific certified reagents of 99.93 percent purity as determined by N. H. Suhr of the Mineral Constitution Laboratory). See Iler (1955) for extensive discussions of colloidal silica. Figure 1 shows the pH of acetic-acid-silicate solutions as a function of milliliters of acid added to 10 ml of a constantly agitated silicate solution. The pH of the gel is measured immediately before gelation and, therefore, does not refer to the pH of the semisolid gel material or of the interstitial solution. The quoted pH is assumed to be a close approximation of the average hydrogen ion concentration in the environment of the growing crystals.

The pH of the solutions was determined by a Photovolt pH meter model 115 with a Beckman fiber junction reference electrode (calomel internals) and a Beckman glass electrode (silver–silver chloride internals) capable of measurements within 0.05 pH unit. The arrangement was calibrated in the normal way using various buffer solutions of known pH. Acetic acid was used to gel the sodium silicate solutions because the pH of a silicic acid gel will not change with time only if a weak acid is used (Hurd and Griffith, 1935).

There are several ways, as shown in Figure 2, in which crystals can be grown in a gelatinous medium. The simplest method is to incorporate a solution of one reactant salt in the acid-silicate mixture before gelation occurs and to pour a solu-

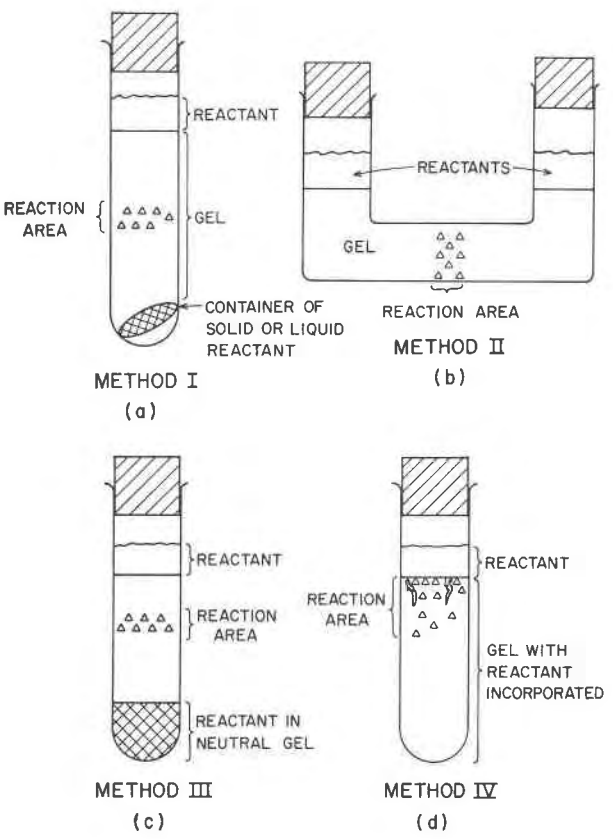

FIG. 2. Some methods for growing crystals in a gel.

tion of the second salt on the gel after gelation (IV). Another method is to form a gel over a packet (*e.g.*, filter paper) of one of the reactants and pour on a solution of the second salt after gelation occurs; reactant concentration effects can only be approximated in this case (I). By a U-tube method (II), both reactant concentrations are well defined and reaction point concentrations can be approximated. The two-gel technique (III) involves preparing a gel containing one of the reactants in the bottom of a test tube as in method IV. However, a second gel, called the reaction gel, is formed over the first gel and a solution containing the second salt is then poured over the reaction gel.

TABLE 1. Some Phases That Have Been Grown by the Gel Technique

Crystals	Method; Reactants	Size (mm)	Remarks
	Sulfates		
$CaSO_4.2H_2O$	IV, $CaCl_2 + H_2SO_4$	5 x 0.5	Twinned crystals
	II, $CaCl_2 + CuSO_4$	30 x 1	High Ca reg. prismatic crys. High SO_4 reg. acicular crys.
	III, $CaCl_2 + H_2SO_4$	5 x 0.5	60°C
$BaSO_4$	II, $BaCl_2 + CuSO_4$	1 x 1	---
$PbSO_4$	II, Pb $(C_2H_3O_2)_2 + CuSO_4$	1 x 1	Used ludox AS for gel
$SrSO_4$	II, $SrCl_2 + CuSO_4$	1 x 1	---
	Chromates		
$PbCrO_4$	II, Pb $(C_2H_3O_2)_2 + K_2CrO_4$	1 x 1	---
	Phosphates		
$Cu_3(PO_4)_2.3H_2O$	IV, $CuSO_4 + H_3PO_4$	---	Spherulites and liesegang rings
$CaHPO_4.2H_2O$	IV, $CaCl_2 + H_3PO_4$	2 x 3	Single crystals; blade-like
$Ca_5(PO_4)_3OH$?	IV, $CaCl_2 + H_3O_4$	---	Liesegang rings & spherulites, & radial crys. clusters at 60°C
	Fluorides		
CaF_2	II, $CaCl_2 + NaF$	<0.01	Spherulitic
SrF_2	II, $SrCl_2 + NaF$	<0.01	---
MgF_2	II, $MgCl_2 + NaF$	<0.01	---
BaClF	II, $BaCl_2 + NaF$	2 x 2	Single crystals
	Tungstates		
$CaWO_4$	II, $CaCl_2 + NaWO_4$	1 x 1	Clear spherulites
	Carbonates		
$CaCO_3$	All, $CaCl_2 + Na_2CO_3$	1 x 1	Calcite, aragonite & vaterite crystals & spherulites
$CaCO_3.H_2O$	IV, $CaCl_2 + Na_2CO_3$ + sugar	1 x 1	Single crystals
$BaCO_3$	II, IV, $BaCl_2 + Na_2CO_3$	1 x 0.1	Sheet-like crystals and spherulites
$SrCO_3$	II, IV, $SrCl_2 + Na_2CO_3$	1 x 0.1	Sheet-like crystals and spherulites
$Nd_2(CO_3)_3.8H_2O$	III, $NdCl_3 + Na_2CO_3$	2 x 1 x 0.1	Lavender plates and spherulites
	Oxides		
Cu_2O	III, IV, $CuSO_4 + NH_2OH.HCl$	0.5 x 0.5	Dark red to transparent yellow cubic crystals
	Chlorides		
CuCl	III, $CuSO_4 + NH_2OH.HCl$	1 x 1	Clear to dark green crystals that decompose in atmosphere
	Iodides		
HgI, Hg_2I_2	IV, $HgCl_2 + KI$	0.2 x 0.2	Liesegang rings of crystals that migrate down tube
PbI_2	IV, $Pb(C_2H_3O_2)_2 + KI$	4 x 0.5	---
	Metals		
Cu	III, $CuSO_4 + NH_2OH.HCl$	2 x 0.5	Needle and 3-d growth, epitaxially on Cu_2O
Pb	All, $Pb(C_2H_3O_2)_2 + Zn$	0.1	Small needles & plates growing on the end of lead "trees"

Calcium carbonate can be prepared by any number of different chemical reactions. The following reaction was utilized in this study:

$$Na_2CO_3 + CaCl_2 \rightarrow CaCO_3 + 2NaCl.$$

Since sodium is part of the gel, it is advantageous to have sodium as part of one of the reactants in order to minimize the amount of foreign cations present. All the chemicals are Fisher certified reagent grade.

The concentrations of the reactants at the point of reaction were calculated and approximated by methods which depended on the method used and which assumed classical diffusion laws. However, the exact concentration is impossible to know except by direct measurement, and the data should be taken to reflect *relative changes* in concentration of the reactants, rather than absolute values of concentration. Impurity cations (Sr, Mg, Ni, and Ba) were added directly to the sodium silicate-acid system before gelation in predetermined concentrations. Hence, the concentrations of these cations are much more accurately known than the absolute reactant concentrations.

The various phases were identified by microscopic observation and X-ray diffraction analysis. Crystals were separated from the gel by vigorous agitation of the final gel and crystal system in a dilute $Ca(OH)_2$ solution. This was carried out repeatedly until all of the gel was removed from the crystals. Crystals to be analyzed by emission spectroscopy (by N. H. Suhr and D. J. Rhine of the Mineral Constitution Laboratory) were further washed alternatively in distilled water and solutions of sodium hydroxide. The spatial distribution of these impurity cations in some of the crystalline products was determined by the use of an ARL electron microprobe operated by E. W. White and G. R. Zechman, Jr., both of the Mineral Constitution Laboratory.

Table 1 lists some of the more important crystals synthesized during the course of this study. Note especially that carbonates, sulfates (McCauley and Roy, 1965), phosphates, chromates, and tungstates

(McCauley and Gehrhardt, 1970), as well as oxides and metals (McCauley, Roy, and Freund, 1969) may be synthesized; the latter by appropriately controlling the oxidation potential of the gel. It seems that by appropriate manipulation of the crystallization environment (Eh, pH, complexing agents, impurity ions, concentration of reactants, temperature, *etc.*) a wide variety of slightly soluble materials may be successfully synthesized into fairly large (0.5 to 1 cm) single crystal size.

Experimental Results

I. Influence of pH and Concentration of Reactants

A. Phase Distribution

Both the pH of the reaction area and the relative and absolute concentration of the reactants have a pronounced effect on the relative percentage of $CaCO_3$ phases that are formed; Figures 3–5 illustrate these results. Using method I (Figure 3) the concentration of $CaCl_2$ was kept constant at about 0.45 molar while varying the molar ratio $CaCl_2$:Na_2CO_3 from 14.5 to 1.45. Primarily to substantiate the method I results, two series of runs were employed using method III; Na_2CO_3 concentration was kept constant at 0.09 molar in one series (Fig. 4) and 0.36 molar (Fig. 5) in another, while varying the $CaCl_2$ concentration from 0.65 to 0.07 molar. The relative percentages indicated in the figures were determined by relatively simple counting techniques under a low power binocular microscope; the percentages (± 10 percent) represent numbers of individual crystals, regardless of size or total weight.

Both aragonite and vaterite formation seem to be a pronounced function of the pH of the reaction area in the gel and, less directly, of the concentration of the two reactants. In particular, pH values roughly between 8 and 10 seem to be most favorable for the precipitation of aragonite and vaterite; reactant concentration effects are observed but unresolved. Further, in all of the test tube runs aragonite crystals formed primarily in regions of the gel closer to the carbonate solution, while vaterite

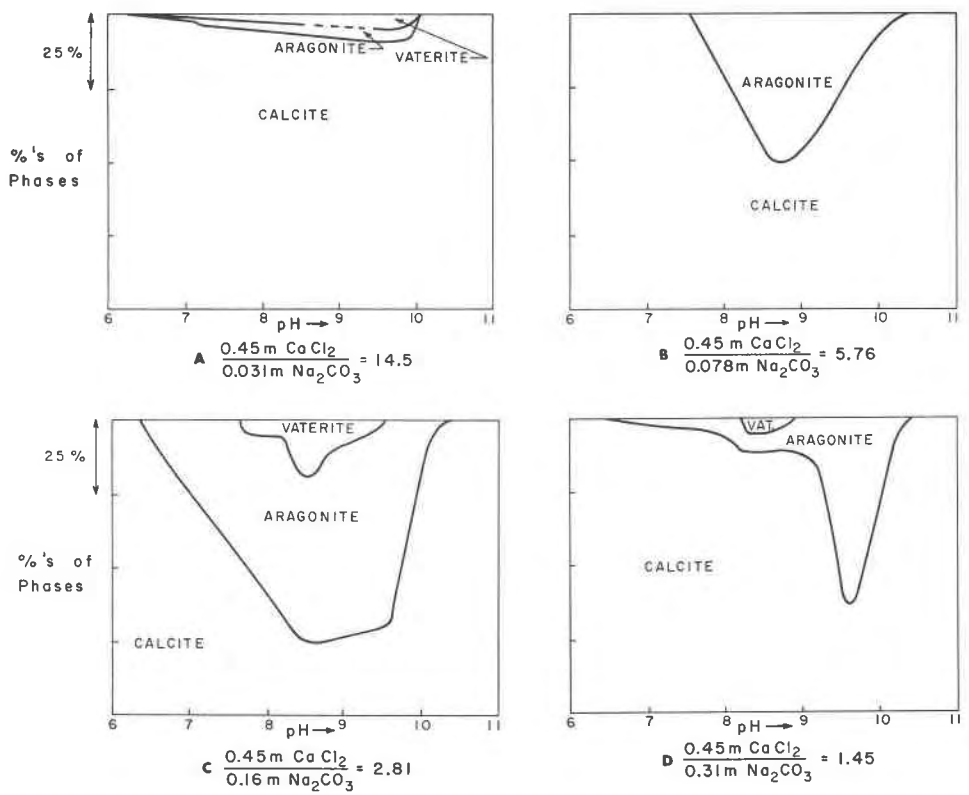

FIG. 3. Percentage of phases formed as a function of reactant concentration and gel pH—using Method I.

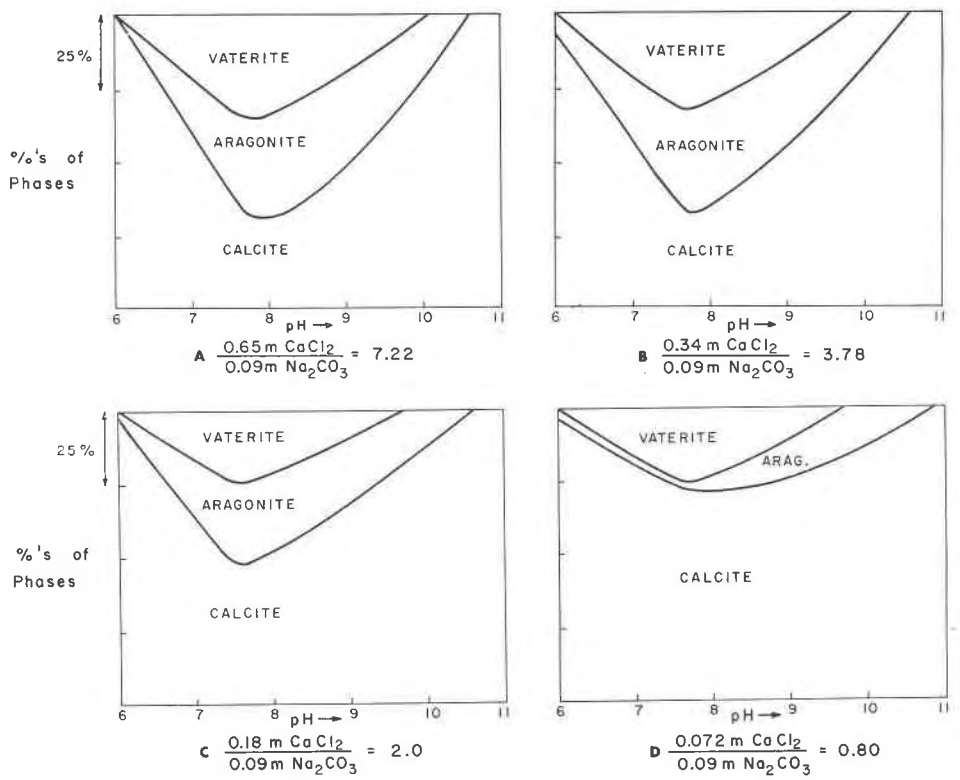

FIG. 4. Percentage of phases formed as a function of reactant concentration and gel pH—using Method III.

preferred areas closer to the calcium solution. In addition, high initial concentrations of both reactants resulted in the formation of a pronounced band of tightly clustered crystals of rapidly grown calcite crystals; smaller concentrations resulted in no discernible band. Figure 6 illustrates these observations on two runs carried out at the same pH. Complete mixing of reactants throughout the gel is restricted in the former case and can substantially modify the interpretations of the results.

For one sequence of runs when the concentration of both reactants was high (Fig. 5a), vaterite precipitated in appreciable amounts at a pH of around 8.00, confirming again that vaterite formation favors high (relative) concentrations of Ca. Additional, but incomplete, studies indicate that vaterite is the predominant phase formed in gels of pH less than 6.0. Schwartz *et al* (1971) have also made observations on pH dependency of the growth of vaterite.

B. Morphology of $CaCO_3$

Calcite formed in various rhombic-type single crystal and polycrystalline aggregates over the whole pH range investigated. Vaterite and aragonite occurred in various crystal clusters and spherulitic morphologies. All morphologies were identified by X-ray powder diffraction. Three distinct morphologic types of calcite were identified:

pH	*Calcite Type*
7 to 9.0 or 9.5	Various single crystal rhombic types;
9.0 to 10.5	feathery—polycrystalline aggregate with rhombic outline;
above 10.5	spicular or spherultic type.

Two types of calcite rhombs are illustrated in Figure 7A: a normal rhomb and a corner growth (hopper-like growth) rhomb resulting from rapid crystal growth. Figures 7B and 7C depict other crystals of calcite and aragonite grown at near neutral pH values. Poisoning of single crystal calcite rhombs takes place in higher pH solutions and results in the formation of feathery and of spicular varieties. The feathery type, a polycrystalline aggregate with a rhombic outline (Figs. 7D and 8G), has a rhombohedral core or nucleus upon which a mass of finely

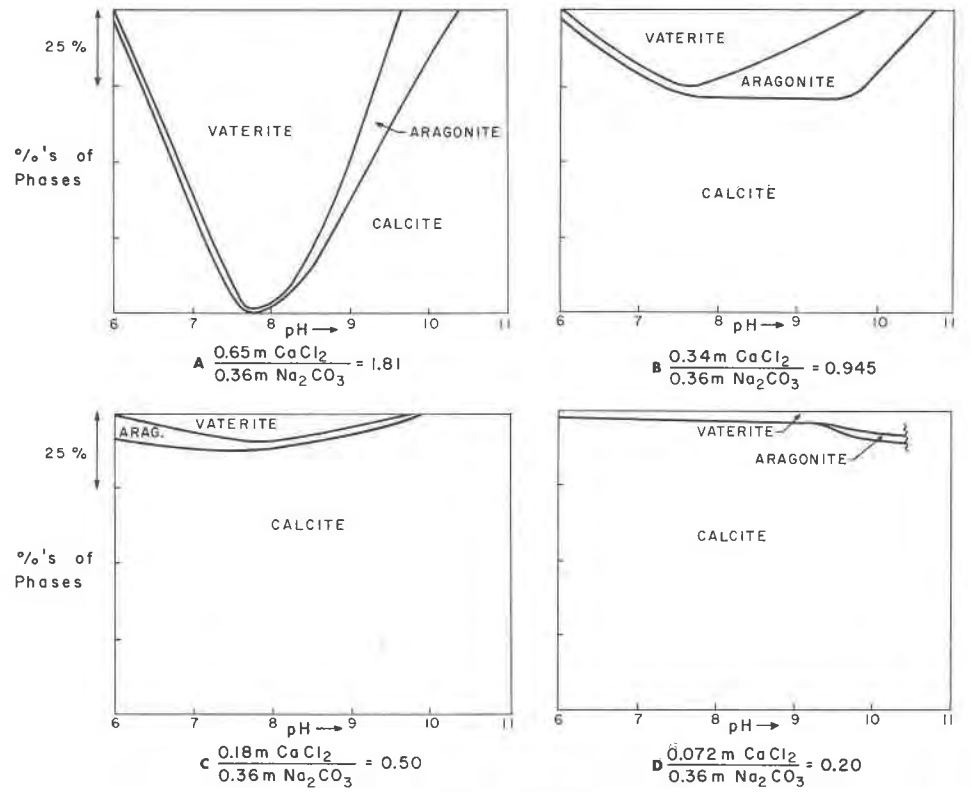

FIG. 5. Percentage of phases formed as a function of reactant concentration and gel pH—using Method III.

acicular crystals nucleate. The rhombic outline is probably preserved because of the symmetrical overgrowth onto the initially formed calcite rhombohedron. Increased poisoning in more basic gels (above 10.5) results in the formation of the spicular type (Figs. 7E and 7F). This particular variety was initially confused with aragonite due to the acicular morphology. Figure 7G and 7H show, respectively, the beginning and intermediate stages of the poisoning of a calcite rhomb which would lead to the crystallization of either the feathery or spicular type.

Figure 8 depicts various observed crystal clusters and spherulitic-like morphologies of aragonite and vaterite; neither precipitated as isolated single crystals. Again more nearly single crystalline material formed at low pH values, (Figs. 7B and 7C), whereas in more basic gels spicular-like and dense, finely polycrystalline masses occur (Figs. 8B to 8G and 7F). Figure 8H shows vaterite spherulites formed under the conditions diagrammed in Figure 5A; a botryoidal-like vaterite (not clear spherulites) occur in most runs very near to the $CaCl_2$ solution. Both

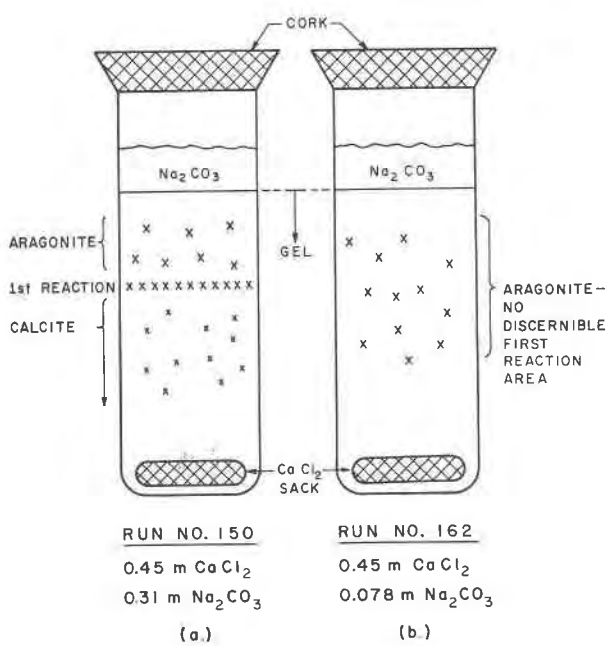

FIG. 6. Spatial distribution of crystals in the gel.

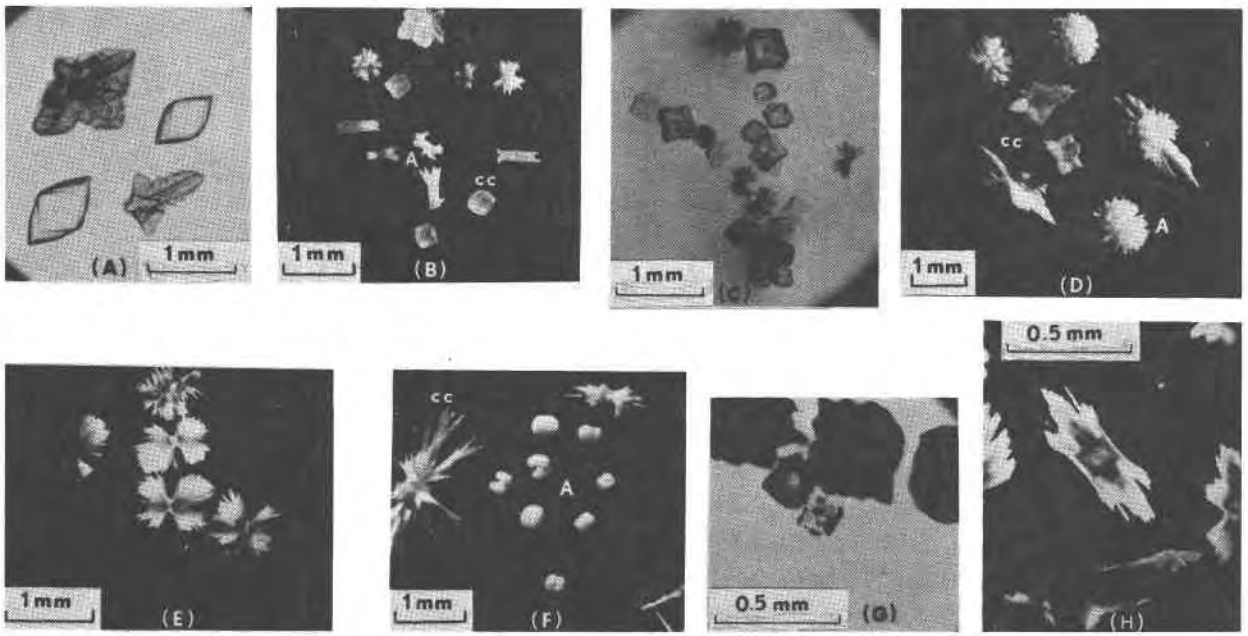

FIG. 7. Various morphologies of calcite: (A) pH = 6.6, (B) pH = 7.3, (C) pH = 7.3, (D) pH = 9.8, (E) pH = 10.5, (F) pH = 10.6, (G) pH = 10.2, (H) pH = 8.9 (CC = calcite, A = aragonite).

the vaterite in Figure 8H and the aragonite in Figure 7F are oolitic in appearance, suggesting a common mechanism.

C. Discussion of Results:

McConnell (1960) has suggested that calcium hydroxide catalyzes the formation of vaterite. The doubled lattice parameters of $Ca(OH)_2$ ($2a$ = 7.19 Å, $2c$ = 9.8 Å) are quite similar to those of vaterite (pseudo-cell) (a = 7.16 Å, c (pseudo) = 8.5 Å, c = 16.94 Å) implying that epitaxy of vaterite on initially formed $Ca(OH)_2$ could be important. However, careful X-ray powder diffraction analysis of hand picked vaterite spherulites revealed that only $CaCO_3 \cdot H_2O$ seemed to be incorporated within the spherulites. The lattice parameters (a = 6.09 Å, c = 7.53 Å, Kohatsu and McCauley, 1973) and powder patterns of $CaCO_3 \cdot H_2O$ are very similar to vaterite. Hence, it appears that epitaxial control of vaterite formation by $CaCO_3 \cdot H_2O$ may be more important than precursor $Ca(OH)_2$ precipitation.

A recent crystal structure analysis of $CaCO_3 \cdot H_2O$ (Kohatsu and McCauley, 1973) showed that its structure is intermediate between those of calcite and aragonite on the one hand, and vaterite on the other. Meyer (1969), in a detailed crystal structure analysis of vaterite, clarified its relationship to the baestnaesite ($RFCO_3$) series of minerals and confirmed the irregularity of the O–O interatomic distances in the CO_3^{2-} group. The similarity of the irregular O–O distances to those in $CaCO_3 \cdot H_2O$ and $NaHCO_3$ (Sharma, 1965) strongly suggests the presence of undetected hydrogen bonding in the vaterite structure. These structure data in conjunction with the fabrication criteria imply that vaterite may not be stoichiometric $CaCO_3$, but rather a calcium rich material ($Ca > CO_3$), with small incorporations of $(OH)^-$, HCO^-_3 or CO_2. One other possibility is that some Na^+ substitutes for Ca^{2+}, allowing for the substitution of $(OH)^-$ or $(HCO_3)^-$.

Figure 9 is a somewhat schematic representation of the relative concentration of various carbonate species and the solubility of $CaCO_3$ as a function of pH; in a strict sense this figure is valid only for very dilute solutions. Freiser and Fernando (1963) show how effective equilibrium constants vary as a function of ionic strength:

$$pK_i' = pK_i - \frac{N\sqrt{\mu}}{1 + \sqrt{\mu}}$$

where μ = ionic strength,
N = integer depending on the electrolyte,
pK = equilibrium constant, and
pK′ = effective equilibrium constant in high μ solutions.

For H_2CO_3, N = 1 for pK_1, and N = 2 for pK_2. As an example of the calculation, when μ = 4.6 the pK_2 for carbonic acid is 8.95, compared to 10.33 for very dilute solutions. This new point corresponds closely with the beginning of poisoning of the calcite rhombs. Hence, the abrupt decrease in solubility of $CaCO_3$ results in more rapid crystallization and the formation of the feathery and spicular varieties of calcite.

It should also be noted, however, that $SiO_2 \cdot 2H_2O$ (H_4SiO_4) becomes much more soluble in highly basic solutions. For example, pK is 9.7 for the reaction $H_4SiO_4 \rightleftarrows H^+ + H_3SiO_4$, a point where the solubility of SiO_2 increases appreciably. Therefore the change in morphology of calcite may also be related to the decreasing inertness (increasing solubility) of the silica gel.

Wood and Holliday (1960) discuss the instability of the HCO_3^- species in a heated aqueous solution of carbonic acid open to the atmosphere:

$$2HCO_3^-(aq.) = H_2O + CO_2\uparrow + CO_3^{2-}.$$

Since CO_2 escapes from this system, essentially the

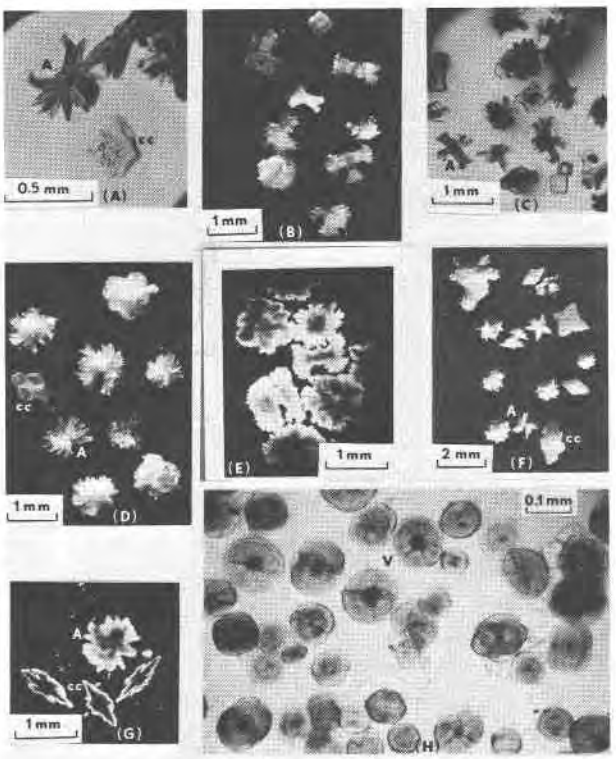

FIG. 8. Various morphologies of aragonite and vaterite: (A) pH = 7.3, (B) pH = 8.9, (C) pH = 8.9, (D) pH = 9.3, (E) pH = 9.3, (F) pH = 9.6, (G) pH = 9.6, (H) pH = 7.5, 0.36 M Na_2CO_3, 0.65 M $CaCl_2$. (CC = calcite, A = aragonite, V = vaterite).

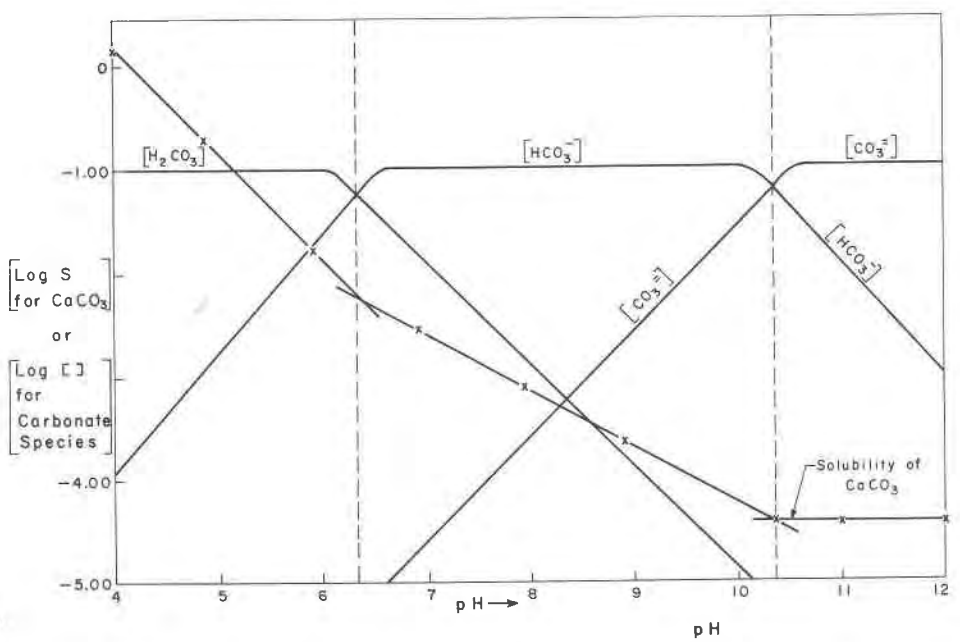

FIG. 9. Slightly schematic solubility diagram for $CaCO_3$.

same effect can be generated by raising the pH of an HCO_3 solution:

$$HCO_3^- = H^+ + CO_3^{2-}.$$

Hence, *in vitro* aragonite formation seems to depend on the presence of abnormally high concentrations of CO_3^{2-} with respect to the predominant HCO_3^- species.

Calcium bicarbonate [$Ca(HCO_3)_2$] exists in solution, but no solid of this composition is known, although both $CaCO_3 \cdot H_2O$ and vaterite may bear a relation to this hypothetical material. Formation of $CaCO_3$ in a bicarbonate solution involves the ejection of a proton (H^+) from the growing crystal to maintain charge balance in the solid:

$$Ca^{2+} + HCO_3^- = CaCO_3\downarrow + H^+.$$

Nancollas and Purdie (1964) point out that it is important to make allowance for these complexes (*i.e.*, $CaHCO_3^+$) in crystal growth rate experiments; this was confirmed for $CaCO_3$ precipitation by Bischoff and Fyfe (1968). McCauley and Roy (1965) also suggested this as an important kinetic consideration. Hence, it is expected from purely kinetic arguments that appreciable amounts of HCO_3^- will be incorporated into a rapidly enlarging $CaCO_3$ nucleus. The amount of entrapment must be dependent upon the nucleation rate and the concentration of HCO_3^-. Nucleation rate is that rate operative in a crystal nucleus before the critical nucleus size is achieved and crystal growth takes over. Therefore, the preceding arguments indicate that for certain pH regimes (or critical mole ratios of CO_3^{2-} to HCO_3^-) the nucleation rate and HCO_3^- concentration are sufficiently high to result in appreciable entrapment of the latter into $CaCO_3$. This entrapment would seem to favor the substitution of Na^+ for Ca^{2+} to balance the excess positive charge caused by the substitution of a HCO_3^- for a CO_3^{2-} group.

Charge imbalance calculations (Pauling, 1929) would seem to indicate that appreciable substitution of HCO_3^- and Na^+ should favor a nine-fold coordination of the cation by oxygen as in aragonite, thus leading to the preferential growth of aragonite-like nuclei rather than calcite. Hence, aragonite is suggested to be a function of proton entrapment, which can be controlled by the pH of the precipitation medium.

Direct evidence for the presence of protons in aragonite formed by this mechanism is hard to obtain. Buerger (1961) has indicated that water analyses on natural calcite and aragonite reveal that aragonite is always higher in water than is calcite. Recently, Kinsman (1970) has shown that aragonite seems to incorporate abnormally high

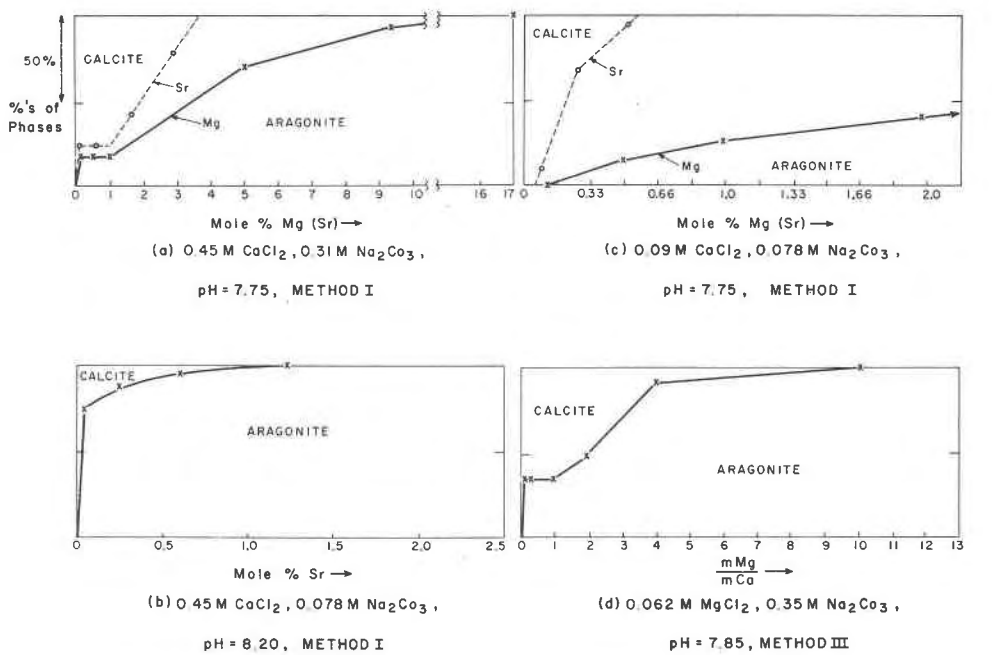

FIG. 10. Percentage of calcite and aragonite as a function of Sr and Mg impurity concentration.

levels of Na^+. In the present work, infrared absorption spectra for aragonite formed by control of pH exhibit a weak band indicative of HCO_3^-. Finally, the proximity of aragonite formation to the carbonate solutions further affirms the proposed mechanism.

II. Influence of Impurity Ions

A. Phase Distribution

The presence of strontium, magnesium, and nickel in the reaction medium favors the formation of aragonite, whereas barium impurities favor vaterite. Figure 10 summarizes the results with strontium and magnesium. It can be seen that the percentage of aragonite formed is directly dependent on the concentration of the impurity ions and on the concentration of the reactants. Note the dependence of the strontium effect on the relative concentration of the reactants, aragonite formation being controlled by strontium more easily when the carbonate concentration was much less than the calcium concentration. Further, strontium always seems to be more effective than magnesium in the formation of aragonite. Figure 10d illustrates the effect of the relative concentration of calcium and magnesium ions on aragonite formation. In this series of runs the concentration of Mg was held constant, while the concentration of calcium was varied, yielding a total crystal yield which decreased appreciably with decreasing Ca concentration.

The preceding results, however, must again be interpreted in regard to Figure 6 which shows that high concentrations of reactants result in very large numbers of nuclei and ensuing rapid growth; low concentrations of reactants have the opposite effect. For practically all of the impurity experiments, calcite formation (when it occurred) was primarily relegated to areas in the gel closer to Ca.

Figures 11A, B, and C are reflected light, plane transmitted, and crossed polarized light photomicrographs, respectively, of calcite crystals (distorted rhombs) and aragonite spherulites grown in the presence of Mg. Calcite and aragonite formed in the runs summarized in Figure 10d are illustrated in 11D. In all of the impurity-generated aragonite spherulites, an optically distinct nucleus (core) was detected with the petrographic microscope. Powder X-ray diffraction analysis of hand picked spherulites (Table 2) revealed the presence of $SrCO_3$ in Sr induced aragonite, but no identifiable phase within

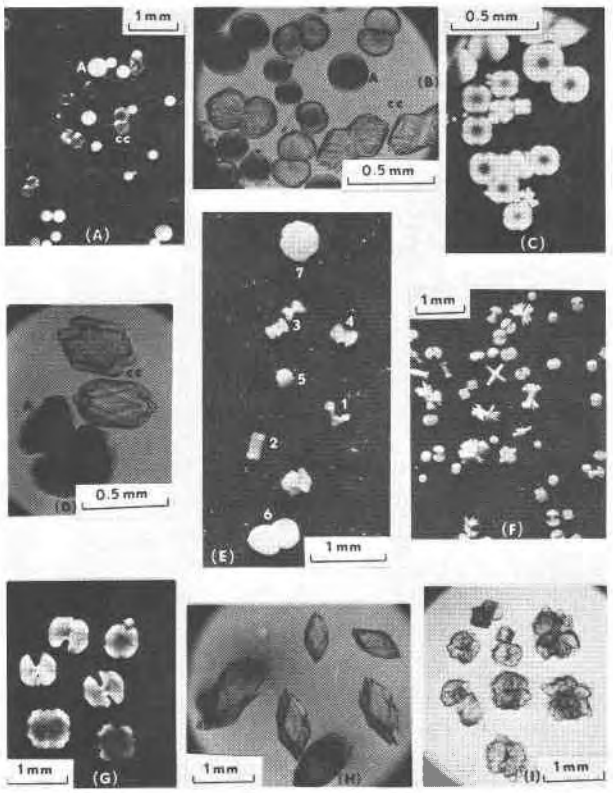

FIG. 11. Influence of impurity ions on the morphology of calcite and aragonite: (A,B,C) 8.92 m% Mg, (D) 0.16 M Ca, 0.06 M Mg, (E) 2.5 m% Sr, (F) 8.9 m% Ni, (G,H) 2.0 m% Ni, (I) 2.0 m% Ba. (CC = calcite, A = aragonite).

the Mg-aragonite. No foreign phase was found even by X-ray analysis of Mg-aragonite spherulites with their outer surfaces dissolved away.

Several Sr-aragonite spherulites were cut in half and examined with an electron microprobe. Figure 12 depicts Ca and Sr X-ray images of a "twinned" spherulite showing $SrCO_3$ at the center of the spherulite. An underexposed electron back scatter

TABLE 2. Percentage of Phases and Sr Partition Coefficients

Run #	Mole % Sr in gel*	% Arag.	%SrCO**	Mole %*** Sr in Arag.	D_{Sr}-A	Mole % Sr in CC	D_{Sr}-CC
160	2.50	100	20	19.05	4.45	-	-
161	1.25	100	15	18.03	7.89	-	-
162	0.63	90	15	10.71	8.70	2.88	2.14
283	0.25	85	10	4.29	8.18	1.22	2.26
163	0.13	85	-	0.07	2.50	1.20	3.78
284	0.05	75	-	-	-	0.04	0.36

*pH = 8.2, 0.078 M Na_2CO_3, 0.38 M $CaCl_2$, method I
**estimated by X-ray powder diffraction of crushed aragonite spherulite
***emission spectroscopic analyses

photograph (12A) shows a small poisoned prismatic crystal of $SrCO_3$ in the center of the spherulite.

A group of hand picked Sr-aragonite spherulites in various stages of development (Fig. 11E) illustrate the proposed mechanism of formation. Early stages of $SrCO_3$ formation and subsequent poisoning are labeled 1–4, while final development of various shaped spherulites are numbered 5–7. This is schematically represented in Figure 13.

Similarly, Mg-aragonite spherulites were sectioned and analyzed with an electron microprobe. A Mg-rich phase was found in the center of the spherulites, but unequivocal identification was not possible. Figure 14A, an electron back-scatter photograph of three joined spherulites, indicates the non-Ca phase at their centers. A Mg X-ray image of this material (14B) showed this to be a Mg-rich phase of very small size as compared to the relatively large $SrCO_3$ nucleus. Exposing these small Mg-rich nuclei for microprobe analysis proved to be extremely difficult and was carried out successfully on only two occasions. These data indicate that the influence of Mg is in terms of the formation of a certain number of nuclei and *not* on the poisoning of calcite crystals, as suggested by Lippmann (1960) and reaffirmed by Bischoff (1968a).

The influence of Ni on the precipitation of $CaCO_3$ is directly analogous to that of Mg, as expected from crystal chemical considerations. Nickel, however, had adverse effects on the gel, limiting this part of the study. Figure 11F is a reflected light photomicrograph of Ni-aragonite spherulites and calcite crystals; the Ni-aragonite spherulites have cores similar to $SrCO_3$ (Fig. 11G). Incorporation of Ni into calcite crystals (Fig. 11H) produces a pale green color.

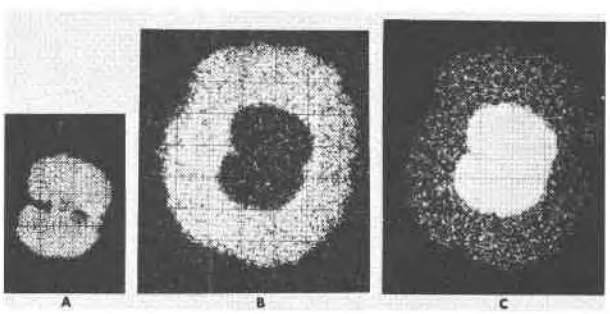

FIG. 12. Electron probe X-ray and electron back scatter photographs of a Sr induced aragonite spherulite: (A) electron back scatter, (B) Ca X-ray scan, (C) Sr X-ray scan. Each division is 36 μm.

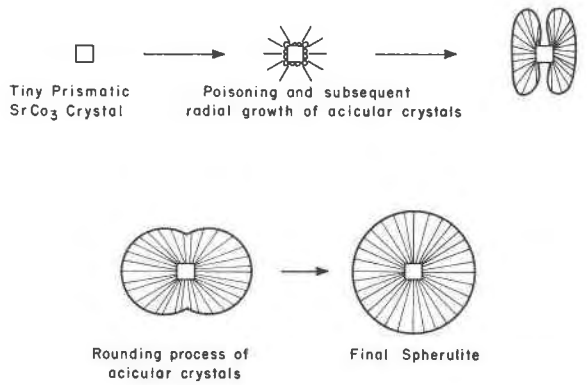

FIG. 13. Schematic representation of formation of aragonite spherulite.

Barium contaminants in the gel favor the formation of isolated (non-overgrown) $BaCO_3$ spherulites and vaterite, and quite drastically alter the calcite morphology; the latter effect can be seen in Figure 11I. As with nickel, however, barium produced adverse effects on the gel. In general, though, large concentrations of Ba in the reaction media (>0.1 molal) resulted in the formation of calcite and witherite ($BaCO_3$), while concentrations less than that resulted in no witherite and various amounts of calcite and vaterite. Apparently $CaCO_3$ cannot overgrow on witherite for these conditions, as it can on strontianite.

Hydrogen ion activity alters the effects of the various impurity cations on the formation of aragonite and vaterite, but no definitive trends were noted. The precipitation of the various hydroxides is one obvious consequence which must be reckoned with. Occasionally in high pH gels addition of the impurity cations caused a milky-like appearance in the gel; this was thought to be either locally polymerized gel or the hydroxide.

B. Partition of Impurity Cations Between Gel Solution and Precipitate

Full understanding of the effect of impurity cations on the precipitation of $CaCO_3$ in silica gel requires a concurrent complementary study on the solid/liquid and solid/solid partition coefficients. The magnitude of such an undertaking is considerable and, therefore, only preliminary results from a modest attempt are reported here. X-ray powder diffraction and emission spectroscopic techniques were utilized to analyze for trace and minor impurities in the solid phases. The different phases and, in some cases, various morphologies of calcite

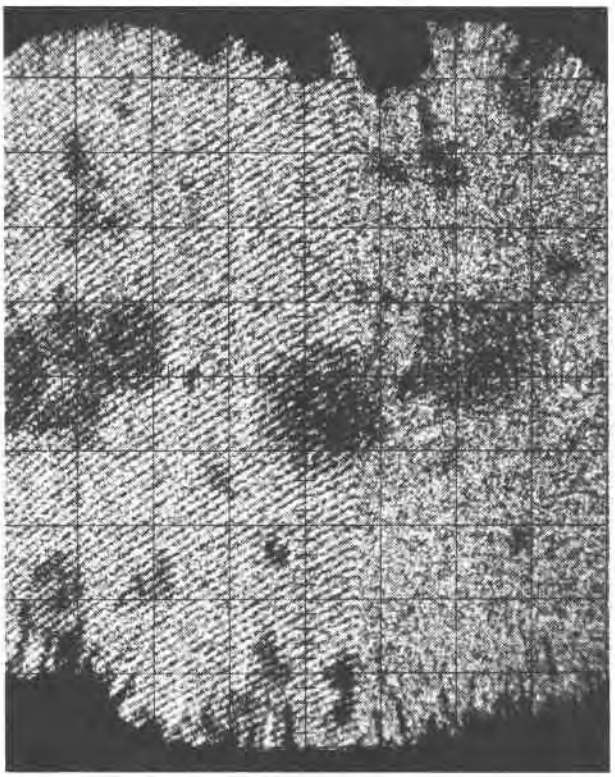

A

and aragonite were hand picked, repeatedly cleaned, and analyzed separately. Partition (distribution) coefficients (D) were calculated according to the homogeneous distribution law as defined by McIntire (1963):
where,

$$D = \frac{Tr_s/Cr_s}{Tr_l/Cr_l}$$

Tr_s = trace component (moles) in solid,

Cr_s = carrier component in solid = 100%—mole % of trace component,

Tr_l, Cr_l = similar concentrations in solution;

and,

D_{Sr}-A = partition coefficient of Sr in aragonite, D_{Sr}-CC = partition coefficient of Sr in calcite, and D_{Mg}-A, D_{Mg}-CC = identical values for Mg.

For this study D is employed as an *effective* partition coefficient, rather than an equilibrium one. Any comparison of these values to equilibrium ones is discouraged; rather, they should be utilized for internal comparison only until they can be meaningfully normalized to equilibrium values. Further, all the analyses showed various amounts of sodium and silicon, but these were neglected in the calculations for the sake of simplicity.

Table 2 lists a representative sampling of partition coefficients measured for Sr in aragonite and calcite. Grand means for *all* analyses (including many not listed in the table) showed the expected results:

$$D_{Sr} - A = 4.37\,\sigma = 2.35$$

$$D_{Sr} - CC = 1.04\,\sigma = 1.08$$

Many factors collaborate to complicate the partition data. First, the partition of Sr into the various solids is a function of pH, since precipitation of the hydroxide will alter the epitaxy and incorporation mechanisms. For example, D_{Sr}-A at a pH of 6.6 is 25, whereas at pH 8.2 D_{Sr}-A is 3. Second, various morphologies of calcite incorporate significantly

B

FIG. 14. Electron probe X-ray photographs of Mg induced aragonite spherulite: (A) Ca X-ray scan, (B) Mg X-ray scan. Each division is 36 μm.

different amounts of Sr—averaging 1.7 mole percent Sr in reaction area crystals and 0.9 in clear, undistorted rhombohedra. Third, low concentrations of reactants favor high Sr incorporations in aragonite, whereas high concentrations favor high Sr incorporations in calcite. Finally, it must also be noted that D_{Sr} is quite dependent on the relative percentage of simultaneously precipitating phases.

The data obtained on the effect of Sr on the precipitation of $CaCO_3$ have reaffirmed the important concept that partition coefficients should reflect the amount of impurity cations in *crystalline solution*. Hence, the presence of $SrCO_3$ nuclei inclusions will distort the results if only bulk analyses are carried out. Only procedures such as X-ray powder diffraction, which measure the *true* amount in solution, can measure equilibrium partition coefficients.

In contrast to the incorporation of Sr into $CaCO_3$, Mg showed no obvious overall preference for either calcite or aragonite. Further, some calcite crystals growing in the presence of Mg had the best transparency of any calcite grown in this study. The amount of Mg incorporated into calcite should depend on the relative and absolute Mg and Ca concentrations. The data in Table 3, however, indicate that Mg incorporation into calcite is more dependent on the relative percentages of calcite and aragonite nucleated. In other words, large amounts of Mg produce Mg-rich nuclei upon which aragonite can grow epitaxially. This, then, depletes the amount of Mg available for incorporation into calcite. Note that Ca concentration was kept constant for these runs. The data in Table 4 are for a series of runs for which Mg concentration was held constant, while Ca was varied. Both X-ray diffraction and emission spectroscopic analyses are listed for comparison; the former being a more meaningful indication of true crystalline solution. Note also that the amount of Mg in calcite can be increased, for constant Mg concentrations, simply by decreasing the Ca concentration. However, as soon as aragonite nucleation increases, less Mg will be available for incorporation into calcite. The high Mg calcites grown in run #311 are pictured in Figure 11D. All the preceding data strongly indicate that the effect of Mg on the precipitation of $CaCO_3$ is by the nucleation of an Mg-rich phase upon which aragonite can epitaxially grow, and *not* on the poisoning of calcite nuclei.

TABLE 3. Percentage of Phases and Mg Partition Coefficients

Run #*	Mole % Mg in gel	% Arag.	Mole %** Mg in Arag.	D_{Mg-A}	Mole % Mg in CC	D_{Mg-CC}
182	16.7	100	2.4	0.06	-	-
185	9.1	80	3.4	0.15	0.68	0.35
186	4.8	65	0.9	0.08	0.85	0.08
292	1.0	20	1.4	0.65	1.00	0.45
293	0.5	20	2.7	2.53	2.61	2.50

*pH ≈ 7.8, 0.37 M $CaCl_2$, 0.31 M Na_2CO_3, method I
**emission spectroscopic analyses

TABLE 4. Various Analyses of Mg in $CaCO_3$

Run #*	M Ca	M Mg/M Ca	% Arag.	Mole%** Mg Arag.	Mg CC	Mole %*** Mg CC
310	0.30	0.20	30	0.35	4.9	2.6
311	0.16	0.37	30	-	-	5.5
312	0.06	1.00	30	0.41	5.3	7.5
313	0.03	2.00	50	0.86	11.3	6.5

*pH ≈ 7.8, 0.06 M $MgCl_2$, 0.35 M Na_2CO_3, method III
**emission spectroscopic analyses
***X-ray diffraction analyses

C. Epitaxial Control of Aragonite Formation

Complementary X-ray diffraction and electron microprobe studies proved that aragonite can grow epitaxially on $SrCO_3$ nuclei. MacDonald (1956) calculated that at least 30 mole percent of Sr in $CaCO_3$ was needed to thermodynamically stabilize the aragonite structure in the calcite stability field. However, once aragonite (or an aragonite-like phase) has reached critical nucleus (one which will persist and grow) size, 30 mole percent Sr will no longer be needed since aragonite can easily overgrow onto a Sr-rich aragonite or Ca-rich $SrCO_3$ critical nucleus. From a thermodynamic point of view, formation of the critical nucleus involves an increase in free energy, whereas crystal growth (after nucleation) involves an exponential decrease in free energy and, thus, is a much more favorable thermodynamic step, allowing for the overgrowth of either calcite or aragonite, since there is negligible difference energetically.

A similar mechanism must be operative in the case of Mg, because of the similarity of the spherulites and the presence of a Mg-rich phase in their center. Epitaxial control requires at least two-dimensional structural similarity. The crystal growth of hexagonal KI on pseudo-hexagonal mica is a good example of this. One measure of lattice parameter similarity is the percent misfit. Aragonite and $SrCO_3$ (strontianite) are quite similar (De Villiers, 1971):

	a(Å)	b(Å)	c(Å)
strontianite	5.09	8.36	6.00
aragonite	4.96	7.97	5.74
% Misfit	2.6	4.9	4.5

$$\% \text{ Misfit} = (|a_1 - a_2|/a_2) \times 100,$$

where, a_2 = lattice parameter of nucleus.

Nesquehonite, $MgCO_3 \cdot 3H_2O$, is the most likely candidate as the Mg-rich phase. Davis (1906) was the first to point out that it instead of $MgCO_3$ precipitated from solution under normal conditions. Langmuir (1965) has recently confirmed these findings from precise thermodynamic data. The lattice parameters of nesquehonite (Stephan and MacGillavry, 1972) and aragonite agree quite well if the c parameter of aragonite is doubled:

	a(Å)	b(Å)	c(Å)	β
nesquehonite	5.37	7.71	12.12	90°45′
aragonite	4.96	7.97	11.48	90°
% Misfit	8.3	3.3	5.6	

Therefore, it is proposed that nesquehonite is the Mg-rich phase which nucleates first, allowing for the subsequent epitaxial overgrowth of aragonite. Very similar mechanisms must be operative in the case of Ni, but no nesquehonite-like Ni phase was found.

Applications to Geologic Conditions

The direct applications of these results to geologic environments is to be cautioned, although one can imagine the similarity of precipitation in a gel to precipitation in a thixotropic mud, in certain cave environments, in various types of sea animals where the gel mimics the organic part of the creature (*e.g.* echinoderm spines), in various sedimentary rocks (limestone, shale, *etc*) where diffusion of solutions is slow, *etc*. Nesquehonite, for example is undersaturated with respect to sea water, but *local kinetic interferences* in equilibrium could affect the precipitation of nesquehonite. Further, nesquehonite has not been unambiguously identified in the aragonite spherulites, thus other Mg-phases such as sepiolite (which was critically examined) could be the key phase. Nesquehonite seems to be the most logical, based on an examination on all known Mg-rich phases which could precipitate from these environments. More detailed work is needed to substantiate this conclusion regarding nesquehonite. Follow-up work on the Ni systems might solve the problem since Ni is much easier to detect with an electron probe and the nuclei were bigger than for the Mg-formed aragonites.

The formation of oolites, certain peculiar calcite morphologies, and high Mg-calcites could be conceivably related to some of the observations made in this study. Thermodynamics is a very useful geologic tool, but many observed phenomena escape thermodynamic explanations and their interpretation must be based on kinetic interferences in equilibrium processes. The writers strongly feel that the data presented in this paper might be very usefully applied to certain unexplained geologic occurrences of the various $CaCO_3$ phases, where thermodynamics has failed. Further, the experimental procedures established can allow for much useful follow-up work on $CaCO_3$ (especially on partition of impurity ions) and other slightly soluble inorganic minerals. Other studies carried out on $CaWO_4$ and $Nd_2(CO_3)_3 \cdot 8H_2O$ (McCauley and Gehrhardt, 1970), Cu_2O-Cu (McCauley, Roy, and Freund, 1969), and unreported work on $CaSO_4 \cdot 2H_2O$ (McCauley, unpublished) demonstrate the flexibility of the experimental procedure and its usefulness in studying the effects of precipitation environment on the nucleation, crystal growth, and doping of slightly soluble materials.

Acknowledgments

The authors would like to acknowledge the contribution of Professor Vladimir Vand (now deceased) to this work. He was responsible for re-introducing the very old gel crystal growth technique as a viable mineralogical and materials science tool to the authors and contributed greatly in the preliminary stages of our learning process. The contributions of Dr. James R. Fisher (USGS) in terms of our understanding of aqueous geochemistry and $CaCO_3$ is also gratefully acknowledged. The authors also wish to acknowledge the help of James R. Craig (VPISU) for his critical reading of the manuscript. The study was carried out under ARPA grant SD-132. The authors are also indebted to the Army Materials and Mechanics Research Center for its support in the final stages of this work.

References

Barta, C., and J. Zemlicka (1971) Growth of $CaCO_3$ and $CaSO_4 \cdot 2H_2O$ crystals in gels. *J. Crystal Growth*, **10**, 158–162.

Bishoff, J. L. (1968a) Kinetics of calcite nucleation: Magnesium ion inhibition and ionic strength catalysis. *J. Geophys. Res.* **73**, 3315–3322.

———, and W. S. Fyfe (1968) Catalysis, inhibition and the calcite-aragonite problem I. The aragonite-calcite transformation. *Am. J. Sci.* **266**, 65–79.

——— (1968b) Catalysis, inhibition and the calcite-

aragonite problem II. The vaterite-aragonite transformation. *Am. J. Sci.* **266,** 80–90.

BRICKER, O. P., AND R. M. GARRELS (1967) Mineralogic factors in natural water equilibria. In, *Principles and Applications of Water Chemistry,* S. D. Faust and J. V. Hunter, Eds., John Wiley and Sons, Inc., New York, 449–469.

BUERGER, M. J. (1961) Polymorphism and phase transformations. *Fortschr. Mineral.* **39,** 9–24.

——— (1971) Crystal-structure aspects of phase transformations. *Trans. Am. Crystallogr. Assoc.* **7,** 1–23.

DAVIS, W. A. (1906) Studies of basic carbonates. *J. Soc. Chem. Ind.* **25,** 788–798.

DEKEYSER, W. L., AND L. DEGUELDRE (1950) Formation de la Calcite, Aragonite, et Vaterite. *Bull. Soc. Chim. Belg.* **59,** 40.

DE VILLIERS, J. P. R. (1971) Crystal structures of aragonite, strontianite, and witherite. *Am. Mineral.* **56,** 758–767.

DONNAY, G., AND J. D. H. DONNAY (1953) The Crystallography of Bastnaesite Parisite, Roentgenite and Synchisite. *Am. Mineral.* **38,** 932–963.

FISHER, J. R. (1962) On the formation of calcite and aragonite: A review. *The Netherworld News,* **10,** 103–114.

FISHER, L. W., AND F. L. SIMONS (1926a) Applications of colloid chemistry to mineralogy; Part I. Preliminary report. *Am. Mineral.* **11,** 124–130.

———, AND ——— (1926b) Applications of colloid chemistry to mineralogy, Part II. Studies of crystal growth in silica gel. *Am. Mineral.* **11,** 200–206.

FREISER, H., AND Q. FERNANDO (1963) *Ionic Equilibria in Analytical Chemistry.* John Wiley and Sons, Inc., New York, 334 p.

GOTO, M. (1961) Some mineralo-chemical problems concerning calcite and aragonite with special reference to the genesis of aragonite. *J. Fac. Sci. Hokkaido Univ., Ser. IV,* **10,** 571–640.

HENISCH, H. K. (1970) *Crystal Growth in Gels.* The Pennsylvania State University Press, University Park, Pennsylvania, 111 p.

HOLLAND, H. D., M. BORCSIK, J. MUNOZ, AND V. M. OXBURGH (1963) The coprecipitation of Sr^{2+} with aragonite and of Ca^{2+} with strontianite between 90° and 100°C. *Geochim. Cosmochim. Acta,* **27,** 957–977.

———, H. J. HOLLAND, AND J. L. MUNOZ (1964) The coprecipitation of cations with $CaCO_3$-II. The coprecipitation of Sr^{2+} with calcite between 90° and 100°C. *Geochim. Cosmochim. Acta,* **28,** 1287–1301.

HOLMES, H. N. (1917) The Formation of Crystals in Gels. *J. Phys. Chem.* **21,** 709–733.

HURD, C. B., AND R. L. GRIFFITH (1935) Studies on silicic acid gels V: The determination of the hydrogen ion concentration of the gel mixtures. *J. Phys. Chem.* **39,** 1155–1159.

ILER, R. K. (1955) *The Colloid Chemistry of Silica and Silicates.* Cornell University Press, Ithica, New York, 324 p.

JOHNSTON, J., H. E. MERWIN, AND E. D. WILLIAMSON (1916) The several forms of calcium carbonate. *Am. J. Sci.* **41,** 473–512.

KINSMAN, D. J. J. (1970) Trace cations in aragonite. *Geol. Soc. Am. Abstr. Programs,* **2,** 596–597.

KITANO, Y. (1962) The behavior of various ions in the separation of calcium carbonate from a bicarbonate solution. *Bull. Chem. Soc. Japan,* **35,** 1973–80.

——— (1964) On factors influencing the polymorphic crystallization of calcium carbonate found in marine biological systems. *Recent Researchers in the Fields of Hydrosphere, Atmosphere and Nuclear Geochemistry,* Maruzen Co. Ltd., Tokyo, p. 305–319.

———, AND D. W. HOOD (1962) Calcium carbonate crystal forms produced from sea water by inorganic processes. *J. Oceanog. Soc., Japan,* **18,** 141–145.

KOHATSU, I., AND J. W. MCCAULEY (1973) Evidence of carbonate order-disorder in $CaCO_3 \cdot H_2O$ (abstr.). *Am. Mineral.* **58,** 1102

LANGMUIR, D. (1965) Stability of Carbonates in the System $MgO\text{-}CO_2\text{-}H_2O$. *Jour. of Geology,* **73,** 730–754.

LIESEGANG, R. E. (1896) Chemishe Fernivirkurg. Noch Sep. von vf., Dusseldorf, Verlog von Ed. Liesegang. Phot. Archiv., **21,** 221.

LIPPMANN, F. (1960) Versuche zur Aufklarung der Bildungs-Bedingunger von Calcit und Aragonit. *Fortschr. Mineral.* **38,** 156–161.

MACDONALD, G. J. F. (1956) Experimental determination of calcite-aragonite equilibrium relations at elevated temperature and pressures. *Am. Mineral.* **41,** 744–756.

MCCAULEY, J. W. (1965) *Control of Nucleation, Crystal Growth, and Doping of Various Calcium Carbonate Phases by the Gel Technique.* M.S. Thesis, The Pennsylvania State University, University Park, Pennsylvania.

———, AND R. ROY (1965) Gel-growth of pure and doped $CaCO_3$ (calcite) and $SrSO_4$ single crystals (abstr.). *Am. Ceram. Soc. Bull.* (ab), **44,** 635–637.

———, AND ——— (1966a) Evidence for epitaxial control of $CaCO_3$ phase formation as the mechanism of the influence of impurity ions (abstr.). *Trans. Am. Geophys.* Union, **47,** 202–203.

———, AND ——— (1966b) The effect of pH and concentration of reactants on the crystal growth of $CaCO_3$. *Geol. Soc. Am. Spec. Pap.* **101,** 136.

———, ———, AND H. FREUND (1969) Crystal growth of copper and nonstoichiometric cuprous oxide by the gel technique. *ACCG Conference on Crystal Growth,* National Bureau of Standards, p. 40.

———, AND H. M. GEHRHARDT (1970) *Crystal Growth of* $CaWO_4$ *and* $Nd_2(CO_3)_3 \cdot 8H_2O$ *by the Gel Technique.* AMMRC TR **70-13,** Army Materials and Mechanics Research Center, Watertown, Mass.

MCCONNELL, J. D. C. (1960) Vaterite from Ballycraigy, Larne, Northern Ireland. *Mineral Mag.* **32,** 535–544.

MCINTIRE, W. L. (1963) Trace element partition coefficients —A review of theory and applications to geology. *Geochim. Cosmochim. Acta,* **27,** 1209–1264.

MEYER, H. J. (1969) Struktur und Fehlordnung des Vaterits. *Z. Kristallogr.* **128,** 183–212.

MORSE, H. W., AND J. D. H. DONNAY (1931) Calcite artificielle obtenue par diffusion dans un gel. *Bull. Soc. Franc. Mineral.* **54,** 19–23.

MURRAY, J. W. (1954) The deposition of calcite and aragonite in caves. *J. Geol.* **62,** 481–491.

NANCOLLAS, G. H., AND N. PURDIE (1964) The kinetics of crystal growth. *Chem. Soc. London Quart. Rev.* **18,** 1–20.

NICKEL, H. J., AND H. K. HENISCH (1969) Growth of calcite crystals in gels. *J. Electrochem. Soc.* **116,** 1258–1260.

OXBURGH, U. M., R. E. SEGNIT, AND H. D. HOLLAND (1959) Coprecipitation of strontium with calcium carbonate from aqueous solutions (abstr.). *Bull. Geol. Soc. Am.* **70,** 1653–1654.

PAULING, L. (1929) The principles determining the structure of complex ionic crystals. *J. Am. Chem. Soc.* **51,** 1010–1026.

SCHWARTZ, A., D. ECKART, J. O'CONNELL, AND K. FRANCIS (1971) Growth of vaterite and calcite crystals in gels. *Mat. Res. Bull.* **6,** 1341–1344.

SHARMA, B. D. (1965) Sodium bicarbonate and its hydrogen atom. *Acta Crystallogr.* **18,** 818–819.

SIEGEL, F. R. (1961) Variations of Sr/Ca ratios and Mg contents in recent carbonate sediments of the northern Florida Keys area. *J. Sediment. Petrol.* **31,** 336.

SIMKISS, K. (1964) Variations in the crystalline form of calcium carbonate precipitated from artificial sea water. *Nature,* **201,** 492–3.

STEHLI, F. G., AND J. HOWER (1961) Mineralogy and early diagenesis of carbonate sediments. *J. Sediment. Petrol.* **31,** 358.

STEPHAN, G. W., AND C. H. MACGILLAVRY (1972) The crystal structure of nesquehonite, $MgCO_3 \cdot 3H_2O$. *Acta Crystallogr.* **B28,** 1031–1033.

VAND, V., H. K. HENISCH, AND J. W. MCCAULEY (1963) Growth of single crystals in gels (abstr.). *Acta Crystallogr.* **16,** A137.

WOOD, C. W., AND A. K. HOLLIDAY (1960) *Inorganic Chemistry*. Butterworths, London, 393 p.

WRAY, J. L., AND F. DANIELS (1957) Precipitation of calcite and aragonite. *J. Am. Chem. Soc.* **79,** 2031–2034.

ZELLER, E. J., AND J. L. WRAY (1956) Factors influencing precipitation of calcium carbonate. *Bull. Am. Assoc. Petrol. Geol.* **40,** 140–152.

Manuscript received, December 12, 1973; accepted for publication, April 5, 1974.